Magnetoresistance and plastic dissipation in twinned YBa$_2$Cu$_3$O$_{7-\delta}$ samples

C. Goupil, F. Warmont, M. Hervieu, J. F. Hamet, and Ch. Simon

CRISMAT, 6 Boulevard du Maréchal Juin, 14050 Caen, France

Using electrical transport measurements, we studied the Ohmic plastic dissipation of twinned YBa$_2$Cu$_3$O$_{7-\delta}$ samples with the magnetic field aligned along the **c** axis. The extracted activation energies $U(T,B)$ were analyzed in the framework of a magnetically induced pinning by twin planes. Vortex-antivortex interactions were derived from the magnetic image effect induced by the deformation of the surrounding supercurrents. The presence of twin planes leads to a crossover from a field-independent activation energy (low fields) to a $B^{-0.5}\ln(B)$ dependence (high fields). The observation of this two-step response is compared with similar observations on heavy-ion-irradiated samples. [S0163-1829(99)14425-4]

INTRODUCTION

Since the unit cell of Y-Ba-Cu-O is slightly orthorhombic, twin planes form easily during the growth process. The exact electrical nature of these planes is still a subject of discussion and probably strongly sample dependent. Nevertheless, it is now well known that such extended defects act as strong pinning centers.[1] Many experimental results, magnetic torque,[2] magnetization,[3] and resistivity[4] show a strong increase of the pinning efficiency when the magnetic induction is aligned with the twin planes. Recently, using scanning tunneling spectroscopy,[5] Maggio *et al.* showed the magnetic interaction of the twin boundaries and the vortices.

On the other hand, flux pinning by correlated disorder in superconductors has been the subject of intense investigations[6,7] because of its ability to immobilize vortices, reduce dissipation effects, and create high critical currents. At low temperature, such systems are predicted to form a Bose-glass phase below the so-called Bose-glass temperature T_{BG} where vortices localize on the defects. Above T_{BG} the system melts into a liquid. Many vortex configurations are then expected, depending on the value of the applied field versus the so-called matching field $B_\Phi \simeq d^{-2}\Phi_0$, where d is the average distance between extended defects. If one considers d, the average distance between twin planes, the corresponding matching field is given by $B_\Phi^{\text{twin}} \simeq \Phi_0/d^2$. In the H-T phase diagram, the Bose-glass line $B_{BG}(T)$ is a decreasing function of the temperature and is limited by the value $B_{BG}(T) = B_\Phi$ at low temperature. Thus for $B \gtrsim B_\Phi^{\text{twin}}$, vortices are expected to be in a liquid state, with short-range correlation order. In the limit of vanishing currents, this phase presents an Ohmic response to transport excitations and allows the extraction of an activation energy, $U(T,B)$ which reveals the underlying mechanism of the flux-line depinning. In order to study these mechanisms, we measured the dc transport response $[R(T)$ and $E(J)]$ of two samples in their Ohmic regime.

In the first section, we will present the two studied samples (one single crystal and one thin film) and describe the microscopical analysis and the technical aspects of the transport measurements. The second section will be devoted to the experimental results, while the third section will discuss the observed dependences and consider the interaction of both the twin plane and neighbor vortices. Finally, conclusions will be drawn.

SAMPLES DESCRIPTION

Single crystal

A single crystal of Y-Ba-Cu-O was grown using the pseudoflux method.[8] The electron diffraction (ED) study was carried out using a JEOL 200 CX electron microscope equipped with an eucentric goniometer ($\pm 60°$). The high-resolution electron microscopy (HREM) was performed with a TOPCON 002B electron microscope, having a point resolution of 1.8 Å. Both microscopes are equipped with energy-dispersive spectroscopy analyzers. More than 50 crystallites were characterized, using ED and HREM. The electron diffraction were carried out in order to reconstitute the reciprocal space and to identify the presence of alien phases such as the ''green phase,'' Y$_2$O$_3$ or BaCO$_3$. Every tested crystallite exhibited the expected cell of Y123 phase, without any evidence of precipitate, and no departure from the Y123 composition. The clear splitting of the $hk0$ reflections in the [001] ED patterns confirms the orthorhombic distortion of the cell, and the formation of twin domains. In the present example, the cross shape of the reflections (see enlargement) confirm the existence of two systems possessing perpendicular domains [Fig. 1(a)]. The HREM image [Fig. 1(b)] shows the nature of the twining boundaries (110) and (1$\bar{1}$0), indicated by large white arrows. Two boundaries, (labeled-1 and 2 in the picture) are spaced by approximately 750 Å which is close to the average value observed over all the studied crystallites which is ≈ 800 Å. Also, our sample possesses a T_c value of 91 K which is close to the optimum for Y-Ba-Cu-O samples. One can note the presence of a third perpendicular twin boundary (labeled tb in the white arrow). We notice that most of the imaged twin planes are coherent, without any strain field or specific defects, giving rise to a uniform contrast between the boundaries. This highly regular contrast confirms the good oxygenation of this material since oxygen deficiency generates microstructures and tweed structures.[9,10] The dimensions of the single crystal used for electrical measurement was approximately 1 mm $\times$ 1 mm $\times$ 0.5 mm. Four parallel silver plots were evaporated on the single crystal and gold wires were subsequently glued on using silver paste. The typical contact resistance was on the order of 0.1 Ω.
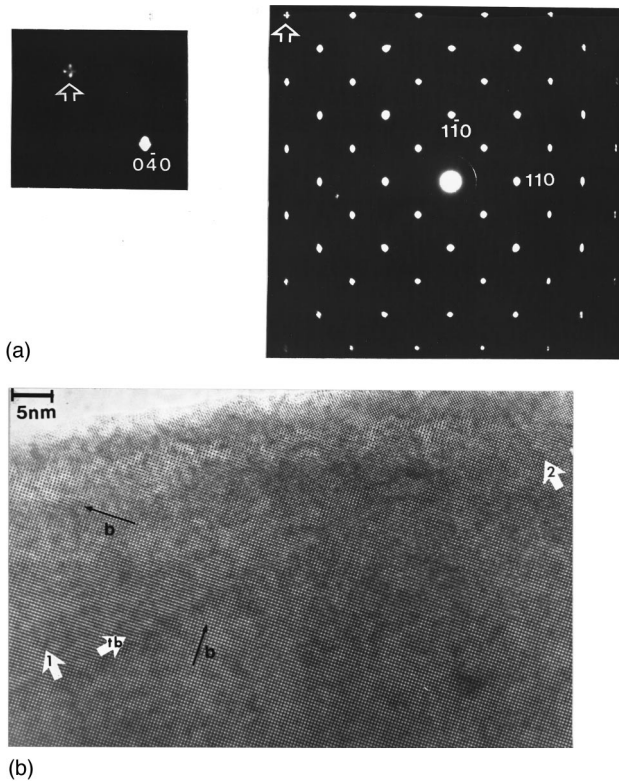
(a)

(b)

FIG. 1. (a) [001] ED pattern of the single crystal. Note the cross shape of the reflexions attesting to the existence of two systems of perpendicular domains. (b) HREM image of the single crystal. The white arrows, labeled 1 and 2, indicate the twin boundaries along (110) and (1$\bar{1}$0). The space between to parallel boundaries is about 750 Å. A third boundary, perpendicular is labeled (tb). Crystallographic b axis are indicated by black arrows.

Thin film

The film was grown using the laser-ablated deposition technique (excimer KrF) on a 3 mm×3 mm (100) MgO substrate. After deposition, the thin-film thickness was 500 Å. The growing conditions and disoxygenation were adjusted to obtain high twin plane density. The [001] ED patterns [Fig. 2(a)] confirm the presence of orthorhombic distortion but the enlargements show that the splitting is smaller than that observed in the single crystal, often resulting in only an elongated shape along [110]* and [1$\bar{1}$0]* planes of the reflections. This effect is usually indicative of a slightly lower oxygen content. As shown in the HREM image [Fig. 2(b)] the average distance between twin planes is ≈ 350 Å which is half the value observed for the single crystal. Strong contrast in the image reveals the width of the twin boundaries (see white arrows) and the presence of important strains inside the structure, which is often the case with high twin planes density. Of same origin is the relatively low $T_c = 87$ K, which reveals a deficiency of the order parameter due the desoxygenation of the sample.

Four gold plots were sputtered on the film and gold wires were glued on using silver paste. The typical contact resistance was of order of 1 Ω. For both samples, electrical transport measurements were achieved with an Adret 103A current source and a Keithley 182 nanovoltmeter. The magnetic field was perpendicular to the **ab** planes. All the $R(T)$ curves (Fig. 3) of the single crystal were driven with a current of
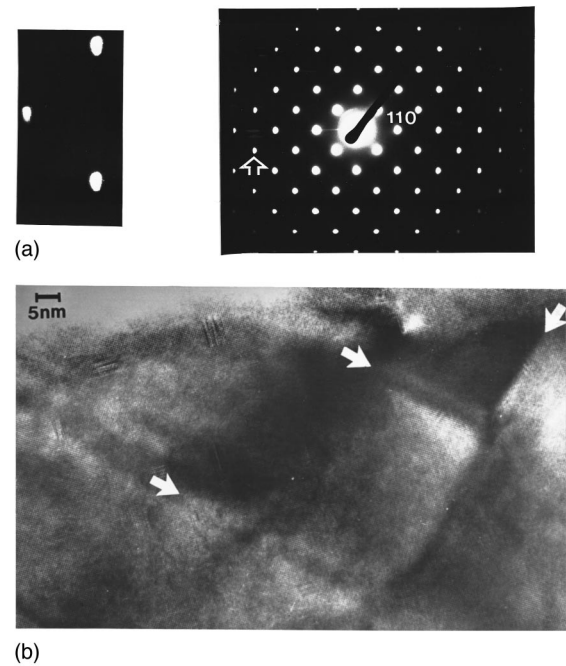

(a)

(b)

FIG. 2. (a) [001] ED pattern of the thin film. Orthorhombic distortion is observed but the splitting is smaller than in the case of the single crystal. This effect is usually connected to a lower oxygen content. (b) HREM image of the thin film. White arrows indicate the twin boundaries. The average distance among them is of order of 350 Å, the strong contrast in the vicinity of the twin boundaries reveals important constraints in these regions.

100 μA to ensure Ohmic response. In the case of the thin film, we recorded isothermal $E(J)$ curves (Fig. 4) and extracted the Ohmic resistivity from the Ohmic lowest currents regimes. These regimes, related to the so-called thermally activated flux flow (TAFF), allowed us to construct the $R(T)$ curves.

RESULTS

In order to get the activation energy of these Ohmic regimes, we considered the following TAFF expression:
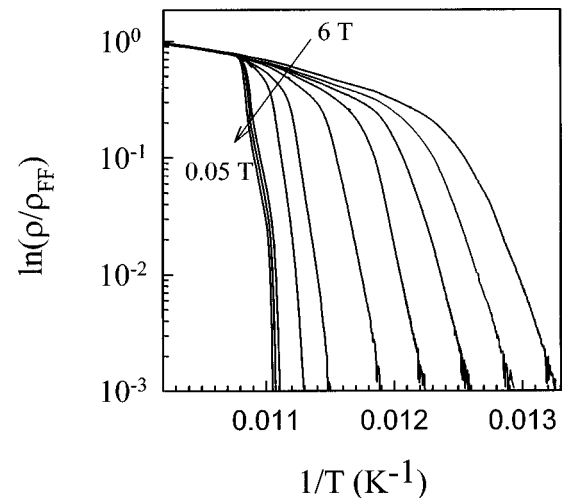

FIG. 3. Single-crystal $R(T)$ results recorded for ten magnetics fields. From left to right: $B = 0.05$, 0.1, 0.2, 0.5, 1, 2, 3, 4, 5, 6.
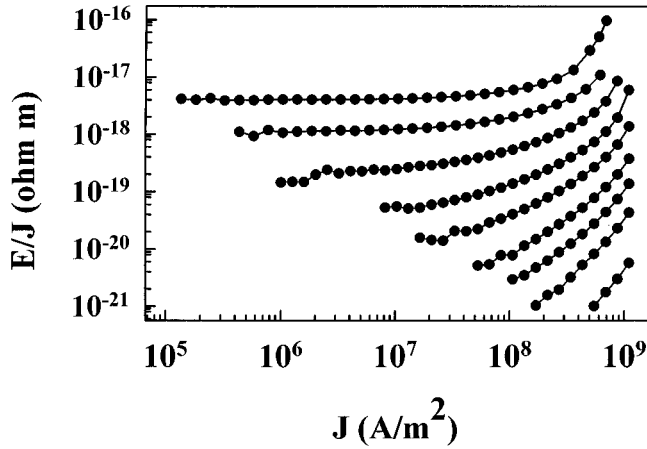
FIG. 4. Thin-film $E(J)$ results recorded at $B = 1$ T for nine temperatures. From left to right: $T = 81.5$, 80.9, 80.2, 79.5, 79, 78.4, 77.9, 77.3, 76.3.

$$\rho_{TAF} = \rho_{FF}(T,B) \exp\left(- \frac{U(T,B)}{kT} \right). \tag{1}$$

One can notice that the flux-flow resistivity ρ_{FF} is a function of both the temperature and the applied induction leading to a complicated determination of $U(T,B) = -kT \ln(\rho_{TAFF}/\rho_{FF}(T,B))$. On the other hand, $\rho_{FF}(T,B)$ determines the ''zero'' activation energy of the process, so we extracted $\rho_{FF}(T,B)$ from the crossover point of all the $R(T)$ curves.

For both samples the activation energies present a linear temperature dependence except near the transition where we observe a slight deviation from linearity at lower $U(T,B)$ (Figs. 5 and 6). This behavior is related to the fluctuation mechanisms which dominate all other dissipation sources when the temperature approaches the T_c of the sample. This study is far beyond the scope of the present paper and will not be presented here. Following these observations, we can write the activation energy in the form:

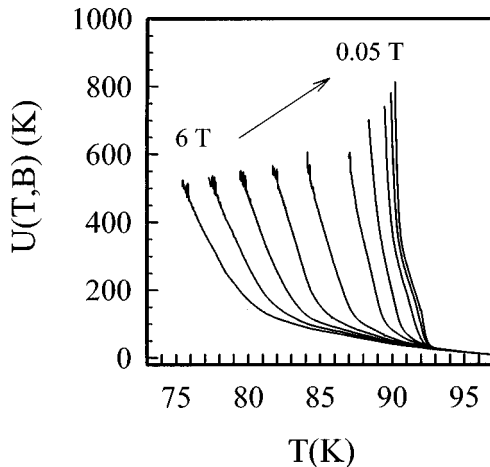$$U(T,B) = U_0(B)\left[1 - \frac{T}{T_c(B)} \right], \tag{2}$$

FIG. 5. Activation energies $U(T,B)$ of the single crystal extracted from the $R(T)$ measurements. From left to right: B (T) $= 0.05$, 0.1, 0.2, 0.5, 1, 2, 3, 4, 5, 6.
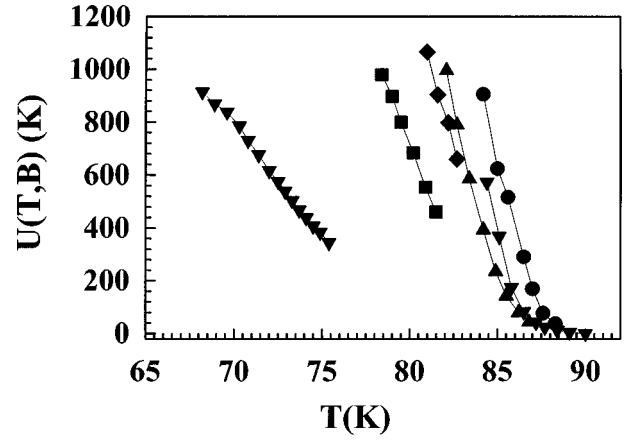

FIG. 6. Activation energies $U(T,B)$ of the thin film extracted from the $E(J)$ measurements. From left to right: $B = (T)= 5$, 1, 0.5, 0.1, 0.05, 0.01.

where $T_c(B)$ is the characteristic temperature above which fluctuation effects dominates.

Using Eq. (2), we can calculate the magnetic dependence from the slope of the $U(T,B)$ curves, and in doing so, one can note the similar behavior of the field dependence of $U(T,B)$ for both the crystal and thin-film samples (Figs. 7 and 8). We observe two distinct regimes ending at a crossover field B_{cr}, which is of order of B_Φ^{twin} for both samples. At low fields, the activation energy is constant. For higher fields, $U(T,B)$ follows a roughly logarithmic dependence which has often been reported previously.[11]

DISCUSSION

In 1991, Feigel'man et al. proposed a logarithmic field dependence of $U(T,B)$ in terms of a dipolar interaction in a two-dimensional (2D) vortex-antivortex nucleated loop.[12] Using a different approach, Jensen[13] and Minhagen[14] interpreted this effect in terms of renormalization of surrounding vortices effect. These points will be developed in the following section.
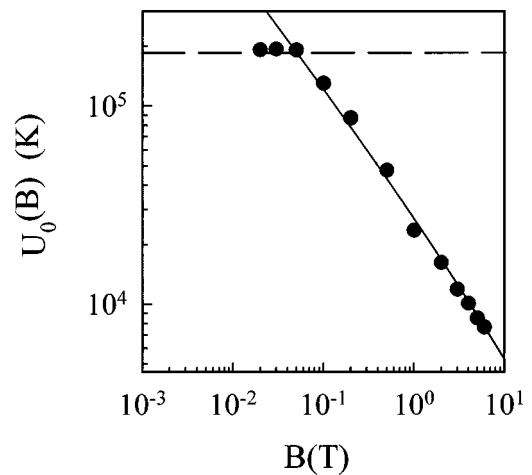

FIG. 7. Magnetic dependence $U_0(B)$ of the activation energy of the single crystal extracted from the $U(T,B)$ results.
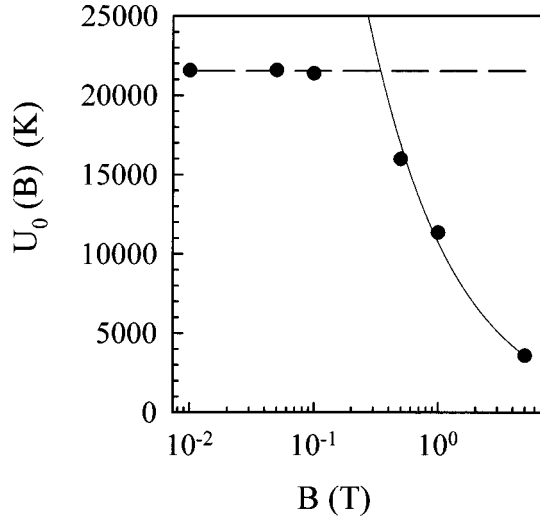
FIG. 8. Magnetic dependence $U_0(B)$ of the activation energy of the thin film extracted from the $U(T,B)$ results.

High-field regime: $B > B_{cr}$

Let us first consider the high-field regime ($B > B_{cr} \simeq B_\Phi^{twin}$). One can observe the quasilogarithmic dependence which is a strong signature of a magnetic interaction between vortices. More precisely, the zero-order Bessel function which describe the radial shape of the induction around a vortex, and consequently the vortex-vortex repulsive energy, reduces to a log function for sufficiently high fields, i.e., small intervortex distances $a_0 \simeq \sqrt{\Phi_0/B}$.[15] Therefore, one see that, in both cases, B_{cr} is much larger than the first penetration field B_{c1}. The observed dissipation in this magnetic-field regime is then governed by the depinning of vortices in the presence of many surrounding neighbors. On the basis of this assumption, Feigel'man proposed a model where the dissipation was driven by the nucleation of a 2D vortex-antivortex loop. This approach is similar to the description of the motion of a rigid flux line inside a lacunary flux-line lattice.[12] With correct cutoff radii, the activation energy is then given by

$$U(T,B) \simeq \frac{\Phi_0^2 D}{16\pi\mu_0 \lambda_{ab}^2} \ln\left(1 + \frac{a_0}{\xi_{ab}(T)}\right), \qquad (3)$$

where D is the sample thickness.

Assuming typical values for the parameters $[\lambda_{ab}(0) \simeq 2000 \text{ Å}, \xi_{ab}(0) \simeq 30 \text{ Å}]$ and where $D = $ thickness, of the sample we get the predicted energy (3). In Table I we compare the calculated and measured values for $B = 1$ T. It is worth noticing that there is a strong disagreement between Feigel'man theoretical predictions and extracted values. Nevertheless, we must point out that neither the electronic

TABLE I. Compared results between measured and predicted energies at 1 T, using the Feigel'man model.

U_0 (1 T)	Prediction	Observation
Thin film	41 500 K	11 000 K
Single crystal	415×10^6 K	26 000 K

anisotropy of the sample nor the presence of twin planes has been taken into account in this description, leading to a large quantitative disagreement.

Low fields regime: $B < B_{cr}$

Let us now consider the low magnetic-field regime ($B < B_{cr} \simeq B_\Phi^{twin}$). The main observation is the absence of magnetic dependence of the activation energy, leading to the conclusion that vortex-vortex interaction cannot contribute to pinning in this low-field regime. More precisely we have $B < B_{cr} \simeq B_\Phi^{twin}$ so the intervortex spacing a_0 is larger than the average distance d between twin planes. In other words, only one vortex can take place between two adjacent twin planes and the vortex-vortex interaction is then screened by the twin planes.

In order to describe in the same model these two regimes, we herein propose a description of the depinning mechanism including anisotropy and twin plane effects.

Plastic dissipation in presence of twin planes

The question of the pinning by twin planes is still controversial, and both the question of the electrical nature of twin plane and the problem of the location of the vortex core inside or outside the twin plane are still unresolved.[5,6,7,16,17] At the present time, no precise observation of pinning by twin planes can conclude for one or the other pinning mechanism. Thus, the interaction between a twin plane and a vortex can be described in two different ways. In the first case, there is a condensation energy gain due to the position of the core inside the planes. On the other hand, this situation indicates that the surrounding supercurrents must flow across the plane where the order parameter is strongly reduced. Consequently, the penetration depth inside the twin plane is strongly increased leading to a vanishing of the corresponding line tension. Therefore, the pinned flux line is expected to be less rigid inside the plane than its neighbors outside the defect.

In the second case, the vortex sits nearby the twin plane and neither the core nor the surrounding currents sit inside the defect. The pinning is then induced by the magnetic image attraction due to the deformation of the supercurrent distribution in the vicinity of the twin plane. One can observe that by this description, the twin plane is assumed to be a normal region with a vanishing order parameter.[5] In other words, and from a magnetic point of view, the vortices feel the twin planes as if they were external surfaces of the sample.

From an experimental point of view, no experiments, especially the magnetic decoration method[18–21] can yield enough resolution to discriminate whether or not the vortex cores and the pinned flux lines sit inside the twin plane. Nevertheless, observations of accumulation desertion of vortices near twin planes using scanning tunneling spectroscopy[5] or magneto-optical patterns of flux distribution,[22] confirm a dominant presence of surface effects such as the Bean-Livingston barrier.[23]

In the following, the vortex-plane interaction will be described by a magnetic image attraction induced by the deformed supercurrent distribution near the twin plane surface
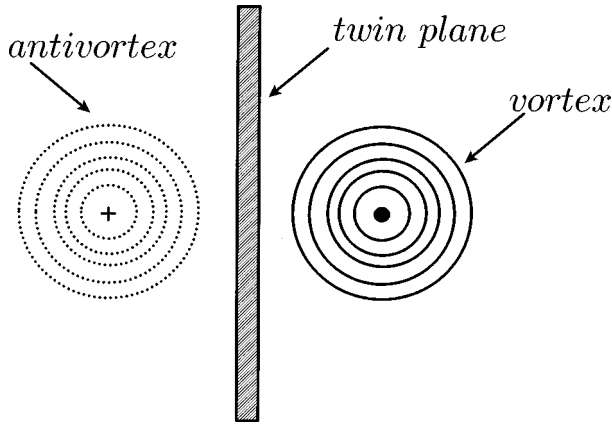
FIG. 9. Schematic description of the magnetic attraction of a vortex by a twin plane. The distortion of the vortex surrounding supercurrents near the twin plane (solid lines) can be analyzed by a magnetic image effect where an antivortex (dashed lines) is in mirror with the vortex leading to an vortex-antivortex attraction.

(Fig. 9). At low fields, this mechanism is easily described by a vortex-antivortex structure with a logarithm attractive dipolar interaction.

Let us now include the effect of the surrounding flux lines and the consecutive constraints. The exact description of this problem in the case of a perfect flux-line lattice is a well-known question which has yet been treated.[15] In the case of anisotropic materials, the line energy and line tension are very well approximated by $\varepsilon_0 \simeq [\Phi_0^2/16\pi\mu_0\lambda_{ab}^2(T)]\ln(\gamma\kappa)$ and $\varepsilon_1(k_z) \simeq [\Phi_0^2/4\pi\mu_0\gamma_{ab}^2(T)]\ln(1+1/k_z\xi_c)$.[15,24] One can notice that the long-range interaction between vortices leads to a dispersive (nonlocal) expression of $\varepsilon_1(k_z)$ where k_z is the wave vector of the line deformation along the **c** axis. In all cases, this approach leads to a relation between longitudinal $l_\parallel$ and transversal $l_\perp$ deformations of a flux line in the presence of neighboring vortices[25] (Fig. 10):

$$l_\parallel = \sqrt{\frac{C_{44}(k_z)}{C_{66}}}\, l_\perp \simeq \frac{l_\perp}{\gamma}. \tag{4}$$
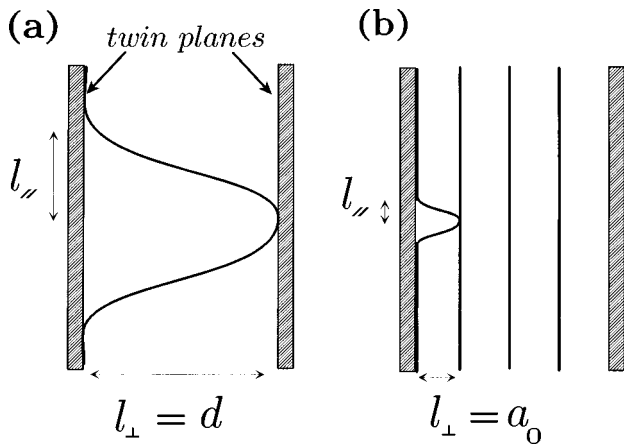

FIG. 10. Schematic description of the twin plane attraction. (a) $B<B_\Phi^{twin}$ so $a_0>d$: the depinning process is driven by the nucleation of a loop with radii $l_\perp=d$ and $l_\parallel \simeq d/\gamma$. (b) $B>B_\Phi^{twin}$ so $a_0<d$: the depinning process is also driven by the nucleation of a loop but the presence of neighboring vortices leads to $l_\perp=a_0$ and $l_\parallel \simeq a_0/\gamma$.

This expression is of particular importance when dealing with elastic and plastic deformations of vortices because the constraints induced by the presence of the surrounding vortices are summarized in one expression. We must mention that similar expressions have been derived by Kramer, from a strong pinning point of view,[26] and from superfluid analogies by Mathieu Simon and Plaçais.[27–29]

Following our pinning description, the activation energy of the depinning process is given by the energy barrier that a vortex segment $l_\parallel$ has to overcome to free it from the attractive potential induced by the twin plane (Fig. 10). Thus, the dipolar interaction is then given by

$$U(T,B) = \frac{\Phi_0^2 l_\parallel}{4\pi\mu_0\lambda_{ab}^2(T)}\ln\left(1+\frac{l_\perp}{\xi_{ab}}\right), \tag{5}$$

where $l_\parallel$ is the vortex segment attracted by the twin plane.

We can now derive the $U(T,B)$ expression for various magnetic-field regimes. For low inductions, $a_0>d$ and one vortex resides between two twin planes. Thus, the transversal jumping length of the line reduces to $l_\perp \simeq d$ and consequently $l_\parallel \simeq d/\gamma$, giving rise to the following equation (Fig. 10):

$$U(T,B<B_\Phi^{twin}) \simeq \frac{\Phi_0^2 d}{4\pi\mu_0\gamma\lambda_{ab}^2}\ln\left(1+\frac{d}{\xi_{ab}}\right). \tag{6}$$

It should be noted that in this case, the activation energy is field independent.

For high inductions, i.e., $B>B_\Phi^{twin}$, we get $a_0<d$ and several vortices sit between two twin planes. Thus the transversal jumping length of the line becomes $l_\perp=a_0$, and consequently $l_\parallel \simeq a_0/\gamma$, which then leads to the following equation:

$$U(T,B>B_\Phi^{twin}) \simeq \frac{\Phi_0^2 a_0}{4\pi\mu_0\gamma\lambda_{ab}^2(T)}\ln\left(1+\frac{a_0}{\xi_{ab}}\right), \tag{7}$$

where the magnetic dependence of $U(T,B) \propto a_0\ln(1+a_0/\xi_{ab})$ differs from the single $\ln(a_0)$ dependence previously described by Feigel'man. Let us mention that such behavior has also been reported in the case of heavy-ion-irradiated samples,[30] but the columnar defects induce strong core pinning which strongly differs, in nature, from the magnetic image attraction induced by twin planes. Consequently, the observed dependence is changed. Nevertheless in both cases, either columnar defects or twin planes, the two lengths $l_\parallel$ and $l_\perp$ seemed to strongly influence the magnetic response of the flux-line lattice.

Following our description, the crossover from the two regimes is expected to occur at $B \simeq B_\Phi^{twin}$. In a more realistic analysis, the dispersion of the distance between twin planes should transform this sharp crossover into a smooth one, which is governed by the smallest values of the B_Φ^{twin} matching field, and is of course related to the largest values of d. We then expect to extract larger d distances from our measurements than the average microscopical value.

Using both expressions (6) and (7), we considered the magnetic-field dependence and fit the different $U_0(B)$ plots. One can notice that the electronic anisotropy and penetration depth cannot be discriminated in such measurements. Therefore, we solve this problem by assuming an average elec-

TABLE II. Physical parameters resulting from the plastic analysis of extracted $U(B)$.

Sample	T_c (K)	d (Å)	B_Φ^{twin} (T)	$\xi_{ab}(0)$ (Å)	$\lambda_{ab}(0)$ (Å)
Thin film	87	770	0.34	25	1930
Single crystal	91	2140	0.044	35	1150

tronic anisotropy for Y-Ba-Cu-O compounds ($\gamma \simeq 6$) which allows us to extract a $\lambda_{ab}(0)$ value from our measurements. The results of these calculations are given in Table II. We notice the excellent agreement between the measured energies and the fitted curves (Figs. 7 and 8). The extracted parameters $\lambda_{ab}(0)$ and $\xi_{ab}(0)$ are also in good agreement with values previously published.[31] From the sample point of view, the lowest critical temperature coincides with the highest in-plane penetration depth, as expected from a reduced superfluid density. On the other hand, the extracted distances between twin planes are more than twice the observed microscopical values. At the present time, this fact is not completely understood therefore, further investigations of the twin plane distribution distances must be undertaken. Also the estimated B_Φ^{twin} is only a crude approximation of the real twin-plane density and its corresponding matching field. Thus, the relation between the microscopical measurement and B_Φ^{twin} is only semiquantitative.

In summary, let us say again that the main parameter in the dissipation process appears to be the electrical anisotropy which governs the value of the longitudinal length $l_\parallel$ (see Fig. 10), and consequently the value of $U_0(B)$. In other words, the presence of twin planes modifies the pinning mechanisms but does not modify the intrinsic nature of the vortex structure. Thus, even in presence of extended defects like twin planes, the depinning mechanisms are governed by the two intrinsic characteristic lengths $l_\parallel$ and $l_\perp$.[32]

CONCLUSION

We studied two Y-Ba-Cu-O twinned samples with different average distance between twin planes. We focused on the Ohmic plastic regime where the vortices are supposed to undergo a liquid state. The extracted activation energies show a classical linear temperature dependence and a two-step magnetic-field dependence. This effect and the values of the energies cannot be explained using the classical Feigel'man 2D model. We derived a plastic description of magnetically pinned vortex by twin planes using a vortex-antivortex attraction by an image effect. This model predicts two regimes separated by a crossover field close to the B_Φ^{twin} matching field. These predictions are in good agreement with the results in terms of magnetic-field dependences and activation energy values.

[1] I. N. Khlustikov and A. I. Buzdin, Adv. Phys. **36**, 271 (1987); A. A. Abrikosov *et al.*, Supercond. Sci. Technol. **1**, 260 (1989); G. Deutcher and K. A. Müller, Phys. Rev. Lett. **59**, 1745 (1987); D. Agassi and J. R. Cullen, Physica C **195**, 277 (1992).

[2] E. M. Gyorgy *et al.*, Appl. Phys. Lett. **56**, 2465 (1990); B. Janossy *et al.*, Physica C **170**, 99 (1990); R. Hergt *et al.*, Phys. Status Solidi A **129**, 1 (1992).

[3] J. Z. Liu *et al.*, Phys. Rev. Lett. **66**, 1354 (1991); U. Welp *et al.*, Appl. Phys. Lett. **57**, 84 (1990); D. L. Kaiser *et al.*, J. Appl. Phys. **70**, 5739 (1990); L. J. Swartzendruber *et al.*, Phys. Rev. Lett. **64**, 483 (1990).

[4] W. K. Kwok *et al.*, Phys. Rev. Lett. **64**, 966 (1990); S. Fleshler *et al.*, Phys. Rev. B **47**, 14 448 (1993); W. K. Kwok *et al.*, Phys. Rev. Lett. **69**, 3370 (1992); J. N. Li *et al.*, Phys. Rev. B **48**, 6612 (1993); W. K. Kwok, J. A. Frendrich, V. M. Vinokur, A. E. Koshelev, and G. W. Crabtree, Phys. Rev. Lett. **76**, 4596 (1996); D. Lopez, E. F. Righi, G. Nieva, F. de la Cruz, W. K. Kwok, J. A. Frendrich, V. M. Vinokur, G. W. Crabtree, and L. Paulius, Phys. Rev. B **53**, 8895 (1996).

[5] I. Maggio-Aprile, Ch. Renner, A. Erb, E. Walker, and Ø. Fisher, Phys. Rev. Lett. **75**, 2754 (1996); I. Maggio-Aprile, Ch. Renner, A. Erb, E. Walker, and Ø. Fisher, Nature (London) **390**, 487 (1997).

[6] D. R. Nelson and V. M. Vinokur, Phys. Rev. Lett. **68**, 2398 (1992); Phys. Rev. B **48**, 13 060 (1993); **48**, 13 060 (1993).

[7] C. Reichhardt, C. J. Olson, J. Groth, Stuart Field, and Franco Nori, Phys. Rev. B **53**, 8898 (1996).

[8] V. Hardy, A. Ruyter, A. Wahl, A. Maignan, D. Groult, J. Provost,

Ch. Simon, and H. Noel, Physica C **257**, 16 (1996).

[9] M. Hervieu, B. Domenges, C. Michel, J. Provost, and B. Raveau, J. Solid State Chem. **71**, 263 (1987).

[10] Z. Hiroi, M. Takano, Y. Ikeda, Y. Takeda, and Y. Bando, Jpn. J. Appl. Phys., Part 2 **27**, L141 (1988).

[11] T. T. M. Palstra, B. Batlogg, L. F. Schneemeyer, and J. V. Waszczak, Phys. Rev. Lett. **61**, 1662 (1988); T. T. M. Palstra, B. Batlogg, R. B. Van Dover, L. F. Schneemeyer, and J. V. Waszczak, Appl. Phys. Lett. **54**, 763 (1989); T. T. M. Palstra, B. Batlogg, L. F. Schneemeyer, R. B. Van Dover, and J. V. Waszczak, Phys. Rev. B **38**, 5102 (1988).

[12] M. V. Feigel'man, V. B. Geshkenbein, and A. I. Larkin, Physica C **167**, 177 (1990).

[13] H. J. Jensen, P. Minhagen, E. Sonin, and H. Weber, Europhys. Lett. **20**, 463 (1992).

[14] P. Minnhagen and P. Olsson, Phys. Rev. B **44**, 4503 (1991).

[15] E. H. Brandt, Phys. Rev. B **48**, 6699 (1993); E. H. Brandt and A. Sudbø, Physica C **180**, 426 (1991).

[16] E. B. Sonin, Phys. Rev. B **48**, 10 487 (1993); E. B. Sonin and M. Krusius, The *Vortex State*, NATO ASI Series C, Vol. 438 (Kluwer, Dordrecht, 1993), pp. 192–230.

[17] J. Groth, C. Reichhardt, C. J. Olson, Stuart B. Field, and Franco Nori, Phys. Rev. Lett. **77**, 3625 (1996).

[18] L. Ya. Vinnikov *et al.*, Solid State Commun. **67**, 491 (1988).

[19] G. J. Dolan *et al.*, Phys. Rev. Lett. **62**, 827 (1989).

[20] V. Grigor'eva, *et al.*, Physica C **195**, 327 (1992).

[21] P. L. Gammel *et al.*, Phys. Rev. Lett. **69**, 3808 (1992).

[22] V. K. Vlasko-Vlasov, L. A. Dorosinskii, A. A. Polyanskii, and V.

I. Nikitenko, Phys. Rev. Lett. **72**, 3246 (1994).

[23] C. P. Bean and J. D. Livingston, Phys. Rev. Lett. **12**, 14 (1964).

[24] A. Sudbø and E. H. Brandt, Phys. Rev. B **43**, 10 482 (1991); Phys. Rev. Lett. **66**, 1781 (1991); **67**, 3176 (1991); **68**, 1758 (1992).

[25] A. I. Larkin and Y. M. Ovchinnikov, J. Low Temp. Phys. **34**, 409 (1979).

[26] E. J. Kramer, J. Appl. Phys. **44**, 1360 (1973); E. J. Kramer and A. D. Gupta, Philos. Mag. **26**, 769 (1972).

[27] P. Mathieu and Y. Simon, Europhys. Lett. **5**, 67 (1988); T. Hoc-quet, P. Mathieu, and Y. Simon, Phys. Rev. B **46**, 1061 (1992).

[28] B. Placais, P. Mathieu, and Y. Simon, Physica C **235-240**, 3049 (1994).

[29] E. B. Sonin, Rev. Mod. Phys. **59**, 87 (1987); Physica B **178**, 106 (1992).

[30] C. Goupil, A. Ruyter, V. Hardy, and Ch. Simon, Physica C **278**, 23 (1997).

[31] G. Blatter, Rev. Mod. Phys. **66**, 1125 (1994).

[32] F. Warmont, C. Goupil, V. Hardy, and Ch. Simon, Phys. Rev. B **58**, 135 (1998).